Discussiones Mathematicae
Graph Theory 43 (2023) 841–858
https://doi.org/10.7151/dmgt.2408

RELATIONSHIP AMONG B1-EPG, VPT AND EPT GRAPHS CLASSES

Liliana Alcón

María Pía Mazzoleni

Universidad Nacional de La Plata, La Plata, Argentina
CONICET

e-mail: liliana@mate.unlp.edu.ar
pia@mate.unlp.edu.ar

AND

Tanilson Dias dos Santos

Universidade Federal do Tocantins, Palmas, Brazil

e-mail: tanilson.dias@mail.uft.edu.br

Abstract

This research contains as a main result the proof that every chordal B_1-EPG graph is simultaneously in the graph classes VPT and EPT. In addition, we describe structures that must be present in any B_1-EPG graph which does not admit a Helly-B_1-EPG representation. In particular, this paper presents some features of non-trivial families of graphs properly contained in Helly-B_1-EPG, namely bipartite, block, cactus and line graphs of bipartite graphs.

Keywords: edge-intersection of paths on a grid, edge-intersection graph of paths in a tree, Helly property, intersection graphs, single bend paths, vertex-intersection graph of paths in a tree.

2010 Mathematics Subject Classification: 05C62.

1. Introduction

Models based on paths intersection may consider intersections by vertices or intersections by edges. Cases where the paths are hosted on a tree appear first in the literature, see for instance [9–11]. Representations using paths on a grid were considered later, see [12, 13, 15].

Let P be a family of paths on a host tree T. Two types of intersection graphs from the pair $< P, T >$ are defined, namely VPT and EPT *graphs*. The *edge intersection graph* of P, EPT(P), has vertices which correspond to the members of P, and two vertices are adjacent in EPT(P) if and only if the corresponding paths in P share at least one edge in T. Similarly, the *vertex intersection graph* of P, VPT(P), has vertices which correspond to the members of P, and two vertices are adjacent in VPT(P) if and only if the corresponding paths in P share at least one vertex in T. VPT and EPT graphs are incomparable families of graphs. However, when the maximum degree of the host tree is restricted to three the family of VPT graphs coincides with the family of EPT graphs [10]. Also it is known that any chordal EPT graph is VPT (see [19]). Recall that it was shown that chordal graphs are the vertex intersection graphs of subtrees of a tree [8].

Edge intersection graphs of paths on a grid are called EPG *graphs*.

In [12], the authors proved that every graph is EPG, and started the study of the subclasses defined by bounding the number of times any path used in the representation can bend. Graphs admitting a representation where paths have at most k changes of direction (*bends*) were called B_k-EPG. In particular, when the paths have at most 1 bend we have the B_1-EPG *graphs* or a *single bend* EPG *graphs*. Sometimes we can refer to a specific path of the representation and its number of bends, for this particular case, we denote by *k-bend* the path or the set of paths that have at most k bends.

A pertinent question in the context of path intersection graphs is as follows. Given two classes of path intersection graphs, the first whose host is a tree and the second whose host is a grid, is there an intersection or containment relationship among these classes? What do we know about it?

In the present paper we will explore B_1-EPG graphs, in particular diamond-free graphs and chordal graphs. We will work on the question about the containment relation among VPT, EPT and B_1-EPG graph classes.

A collection of sets satisfies the *Helly property* when every pairwise intersecting subcollection has at least one common element. When this property is satisfied by the set of vertices (edges) of the paths used in a representation, we get a Helly representation. Helly-B_1-EPG graphs were studied in [5]. It is known that not every B_1-EPG graph admits a Helly-B_1-EPG representation. We are interested in determining the subgraphs that make B_1-EPG graphs that do not admit a Helly representation. In the present work, we describe some structures that will be present in any such subgraph, and, in addition, we present new Helly-B_1-EPG subclasses. Moreover, we describe new Helly-B_1-EPG subclasses and we give some sets of subgraphs that delimit Helly subfamilies.

2. Definitions and Technical Results

The *vertex set* and the *edge set* of a graph G are denoted by $V(G)$ and $E(G)$, respectively. Given a vertex $v \in V(G)$, $N(v)$ represents the *open neighborhood* of v in G. For a subset $S \subseteq V(G)$, $G[S]$ is the subgraph of G induced by S. If $\mathcal{F}$ is any family of graphs, we say that G is *$\mathcal{F}$-free* if G has no induced subgraph isomorphic to a member of $\mathcal{F}$.

A *cycle*, denoted by C_n, is a sequence of distinct vertices $v_1, \ldots, v_n, v_1$ where $v_i \neq v_j$ for $i \neq j$ and $(v_i, v_{i+1}) \in E(G)$, such that $n \geq 3$. A *chord* is an edge that is between two non-consecutive vertices in a sequence of vertices of a cycle. An *induced cycle* or *chordless cycle* is a cycle that has no chord, in this paper an induced cycle will simply be called a *cycle*. A graph G formed by an induced cycle H plus a single universal vertex v connected to all vertices of H is called a *wheel graph*. If the wheel has n vertices, it is denoted by n-wheel.

The *k-sun graph* S_k, $k \geq 3$, consists of $2k$ vertices, an independent set $X = \{x_1, \ldots, x_k\}$ and a clique $Y = \{y_1, \ldots, y_k\}$, and edge set $E_1 \cup E_2$, where $E_1 = \{(x_1, y_1); (y_1, x_2); (x_2, y_2); (y_2, x_3); \ldots, (x_k, y_k); (y_k, x_1)\}$ and $E_2 = \{(y_i, y_j) \mid i \neq j\}$.

A graph is a B_k-EPG graph if it admits an EPG representation in which each path has at most k bends. When $k = 1$ we say that this is a *single bend EPG* representation or simply a B_1-EPG representation. A *clique* is a set of pairwise adjacent vertices and an *independent set* is a set of pairwise non adjacent vertices. A *path* (in the grid) is defined as a finite sequence of consecutive edges $e_1 = (v_1, v_2), e_2 = (v_2, v_3), \ldots, e_i = (v_i, v_{i+1}), \ldots, e_m = (v_m, v_{m+1})$, where $v_i \neq v_j$ for $i \neq j$. A *segment* is a path without bends. The notation $[x_i, x_j] \times \{y\}$ (respectively, $[y_p, y_q] \times \{x\}$), where $i < j$ (respectively, $p < q$), is used to denote the *horizontal segment* (respectively, vertical segment) between columns x_i and x_j (respectively, between rows y_p and y_q), on row y (respectively, column x). In B_1-EPG representations we use $\lrcorner$-path notation and $\llcorner$-path notation to denote the path that has horizontal segment and with bend at right to up, and at left to up, respectively.

Given three 1-bend paths P_1, P_2, P_3 that have at least one segment on the same line L_0 (row or column) of the grid. Let $S_1 = [x_1, x_2] \times \{y\}$ (analogously $S_1 = [y_1, y_2] \times \{x\}$), $S_2 = [x_3, x_4] \times \{y\}$ (analogously $S_2 = [y_3, y_4] \times \{x\}$), $S_3 = [x_5, x_6] \times \{y\}$ (analogously $S_3 = [y_5, y_6] \times \{x\}$) be the segments on L_0, when $x_3 \geq x_2$ (respectively, $y_3 \geq y_2$) and $x_4 \leq x_5$ (respectively, $y_4 \leq y_5$) we say that the segment S_2 (or the path P_2) is *between* S_1 and S_3 (respectively, P_1 and P_3) on the line L_0.

Given an EPG representation of a graph G, we will identify each vertex v of G with the corresponding path P_v of the grid used in the representation. Accordingly, for instance, we will say that a vertex of G covers or contains some

edge of the grid (meaning that the corresponding path does), or that a set of paths of the representation induces a subgraph of G (meaning that the corresponding set of vertices does).

In a B_1-EPG representation, a clique K is said to be an *edge-clique* if all the vertices of K share a common edge of the grid (see Figure 1(a)). A *claw of the grid* is a set of three edges of the grid incident to the same point of the grid, which is called the *center of the claw*. The two edges of the claw that have the same direction form the *base of the claw*. If K is not an edge-clique, then there exists a claw of the grid (and only one) such that the vertices of K are those containing exactly two of the three edges of the claw; such a clique is called *claw-clique* [12] (see Figure 1(b)).

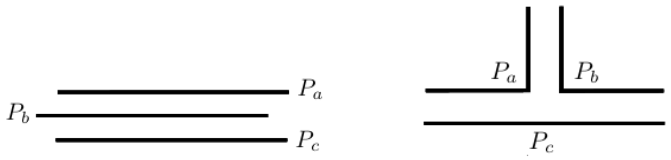

(a) Representation of a clique as edge-clique.

(b) Representation of a clique as claw-clique.

Figure 1. Examples of clique representations.

Notice that if three vertices induce a claw-clique, then exactly two of them turn at the center of the corresponding claw of the grid, and the third one contains the base of the claw. Furthermore, any other vertex adjacent to the three vertices must contain two of the edges of that claw, then the following lemma holds.

Lemma 1. *If three vertices are together in more than one maximal clique of a graph G, then in any B_1-EPG representation of G the three vertices do not form a claw-clique.*

In [3] Asinowski *et al.* proved the following lemma for C_4-free graphs.

Lemma 2 [3]**.** *Let G be a B_1-EPG graph. If G is C_4-free, then there exists a B_1-EPG representation of G such that every maximal claw-clique K is represented on a claw of the grid whose base is covered only by vertices of K.*

We have obtained the following similar result for diamond-free graphs. A *diamond* is a graph G with vertex set $V(G) = \{a, b, c, d\}$ and edge set $E(G) = \{ab, ac, bc, bd, cd\}$.

Lemma 3. *Let G be a B_1-EPG graph. If G is diamond-free, then in any B_1-EPG representation of G, every maximal claw-clique K is represented on a claw of the grid whose edges are covered only by vertices of K.*

Proof. Let K be a maximal clique which is a claw-clique in a given B_1-EPG representation of G. Then there exist three vertices of K which induce a claw-clique K' on the same claw of the grid as K. Assume, in order to derive a contradiction, that a vertex $v \notin K$ covers some edge of the claw. Clearly, v must cover only one of such edges. Therefore v and the vertices of K' induce a diamond, a contradiction. ■

Let Q be a grid and let (a_1, b), (a_2, b), (a_3, b), (a_4, b) be a 4-star centered at b as depicted in Figure 2(a). Let $\mathcal{P} = \{P_1, \ldots, P_4\}$ be a collection of four paths each containing a different pair of edges of the 4-star. Following [12], we say that the four paths form

- a *true pie* when each one has a bend at b, Figure 2(b); and
- a *false pie* when exactly two of the paths bend at b and they do not share an edge of the 4-star, Figure 2(c).

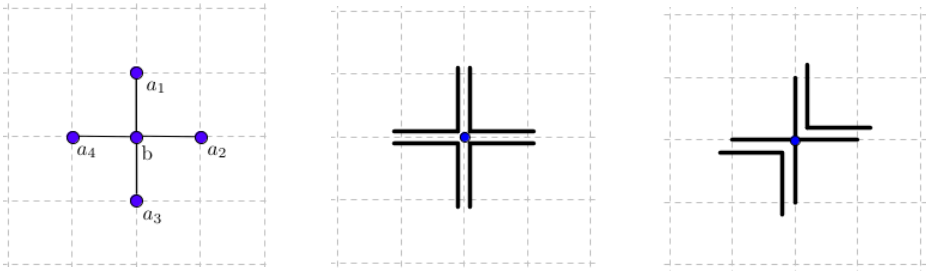

(a) 4-star in grid. (b) True pie. (c) False pie.

Figure 2. B_1-EPG representation of the induced cycle of size 4 as pies with emphasis in center b.

Clearly if four paths of a B_1-EPG representation of G form a pie, then the corresponding vertices induce a 4-cycle in G. The following result can be easily proved. We say that a set of paths form a claw when each pair of edges of the claw is covered by some of the paths.

Lemma 4. *In any B_1-EPG representation of a graph G, a set of paths forming two different claws centered at the same point of the grid contains four paths forming either a true pie or a false pie. Therefore, in any B_1-EPG representation of a chordal graph G, no two maximal claw-cliques of G are centered at the same point of the grid.*

Lemma 5. *Let G be a graph whose vertex set can be partitioned into a non trivial clique K and an independent set $I = \{w_1, w_2, w_3\}$, such that each vertex of K is adjacent to each vertex of I. Then, in any B_1-EPG representation of G, at least one of the cliques $K_i = K \cup \{w_i\}$, with $1 \leq i \leq 3$, is an edge-clique.*

Proof. Assume, in order to derive a contradiction, that the three cliques are claw-cliques. By Lemma 4, they have different centers, say the points q_1, q_2, q_3 of the grid, respectively. Since at least two paths have a bend at the center of a claw, for each $i \in \{1, 2, 3\}$, there must exist a vertex v_i of K such that the corresponding path P_{v_i} turns at the point q_i of the grid. Notice that each one of the three paths P_{v_i} must contain the three grid points q_1, q_2 and q_3. To prove that this is not possible, we will consider, without loss of generality, two cases. First, q_1 is between q_2 and q_3 in P_{v_1}. Then, P_{v_3} cannot turn at q_3 and contain q_1 and q_2. And second, q_2 is between q_1 and q_3 in P_{v_1}. In this case, P_{v_2} cannot turn at q_2 and contain q_1 and q_3; thus the proof is completed. ■

Three vertices u, v, w of a graph G form an *asteroidal triple* (AT) of G if for every pair of them there exists a path connecting the two vertices and such that the path avoids the neighborhood of the remaining vertex [4]. A graph without an asteroidal triple is called AT-*free*.

Lemma 6 [3]**.** *Let v be any vertex of a B_1-*EPG *graph G. Then $G[N(v)]$ is* AT-*free.*

Let C be any subset of the vertices of a graph G. The *branch graph* $B(G|C)$, see [12], of G over C has a vertex set, $V(B)$, consisting of all the vertices of G not in C but adjacent to some member of C, i.e., $V(B) = N(C) \setminus C$. Adjacency in $B(G|C)$ is defined as follows: we join two vertices x and y by an edge in $E(B)$ if and only if in G occurs.

1. x and y are not adjacent;
2. x and y have a common neighbor $u \in C$;
3. The sets $N(x) \cap C$ and $N(y) \cap C$ are not comparable, i.e., there exist private neighbors $w, z \in C$ such that w is adjacent to x but not to y, and z is adjacent to y but not to x; we say that x and y are neighborhood incomparable.

We let $\chi(G)$ denote the chromatic number of G.

Lemma 7 [12]**.** *Let C be any maximal clique of a B_1-*EPG *graph G. Then the branch graph $B(G|C)$ is $\{P_6, C_n$ for $n \geq 4\}$-free, and $\chi(B(G/C)) \leq 3$.*

3. Subclasses of Helly-B1-EPG Graphs

In this section, we delimit some subclasses of B_1-EPG graphs that admit a Helly-B_1-EPG representation. It is known that B_1-EPG and Helly-B_1-EPG are hereditary classes, so they can be characterized by forbidden structures. In both cases, finding the list of minimal forbidden induced subgraphs are challenging open problems. Taking a step towards solving those problems, we describe a few

structures at least one of which will necessarily be present in any B_1-EPG graph that does not admit a Helly representation. In addition, we show that the well known families of block graphs, cactus and line graph of bipartite graphs are totally contained in the class Helly-B_1-EPG.

Let $S_3, S_{3'}, S_{3''}$ and C_4 be the graphs depicted in Figure 4.

Theorem 8. *Let G be a B_1-EPG graph. If G is $\{S_3, S_{3'}, S_{3''}, C_4\}$-free, then G is a* Helly-B_1-EPG *graph.*

Proof. If G is not a Helly-B_1-EPG graph, then in each B_1-EPG representation of G, there is at least one clique that is represented as claw-clique and not as edge-clique. Consider any B_1-EPG representation of G and let K be a maximal clique which is represented as a claw-clique. Assume, without loss of generality, K is on a claw of the grid with base $[x_0, x_2] \times \{y_0\}$ and center $C = (x_1, y_0)$. Denote by $\mathcal{P}_K$ the set of paths corresponding to the vertices of K. By Lemma 2, the grid segment $[x_0, x_2] \times \{y_0\}$ is covered only by vertices of K.

For every $\lrcorner$-path (respectively, $\llcorner$-path) belonging to $\mathcal{P}_K$, we do the following. If the path does not intersect any path $P_t \notin \mathcal{P}_K$ on column x_1, then we delete its vertical segment and add the grid segment $[x_1, x_2] \times \{y_0\}$ (respectively, $[x_0, x_1] \times \{y_0\}$). If after this transformation there is no more $\lrcorner$-paths (respectively, $\llcorner$-paths) in $\mathcal{P}_K$, then we are done since we have obtained an edge-clique. So we may assume that every $\lrcorner$-path and every $\llcorner$-path in $\mathcal{P}_K$ intersects some path $P_t \notin \mathcal{P}_K$ on column x_1 (notice that we can assume is the same path P_t for all the vertices).

Now, if none of the $\lrcorner$-paths belonging to $\mathcal{P}_K$ intersect a path not in $\mathcal{P}_K$ on the line y_0, then we can replace the horizontal part of those paths by the segment $[x_1, x_2] \times \{y_0\}$, getting an edge representation of the clique K. Thus, we can assume there exists at least one $\lrcorner$-path $P_v \in \mathcal{P}_K$ intersecting some path $P_{t'} \notin \mathcal{P}_K$ on line y_0. Analogously, there exists at least one $\llcorner$-path $P_{v'} \in \mathcal{P}_K$ intersecting some path $P_{t''} \notin K$ on line y_0, as depicted in Figure 3. Notice that vertex t' cannot be adjacent to any of the vertices t, v' or t''; and, in addition, vertex t'' cannot be adjacent to t, or v.

Finally, since K is claw-clique, there is a path $P_u \in \mathcal{P}_K$ covering the base of the claw. Depending on the possible adjacencies between u and t' or t'', one of the graphs S_3, $S_{3'}$ or $S_{3''}$ is obtained. ∎

Notice that any bull-free graph is $\{S_3, S_{3'}, S_{3''}\}$-free, so our previous result implies Lemma 5 of [3].

Next theorem has as consequence the identification of several graph classes where the existence of a B_1-EPG representation ensures the existence of a Helly-B_1-EPG representation.

Theorem 9. *If G is a B_1-EPG and diamond-free graph, then G is a* Helly-B_1-EPG *graph.*

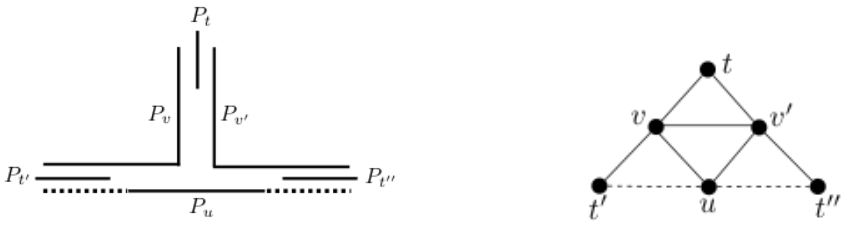

(a) Claw with paths. (b) Subgraph induced by paths.

Figure 3. Reconstruction of the intersection model.

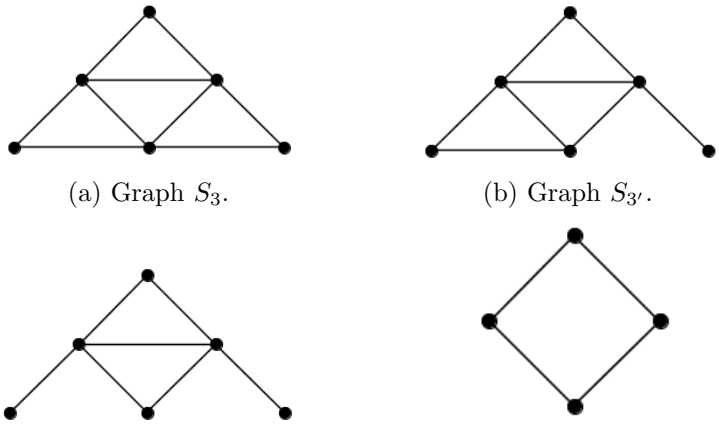

(a) Graph S_3. (b) Graph $S_{3'}$.

(c) Graph $S_{3''}$. (d) Graph C_4.

Figure 4. Graphs on the statement of Theorem 8.

Proof. If G is not a Helly-B_1-EPG graph, then in each B_1-EPG representation of G, there is at least one clique that is represented as claw-clique and no as edge-clique. Consider any B_1-EPG representation of G and let K be a maximal clique which is represented as a claw-clique. Assume, without loss of generality, K is on a claw of the grid with base $[x_0, x_2] \times \{y_0\}$ and center $C = (x_1, y_0)$, similar to the proof of Theorem 8. Denote by $\mathcal{P}_K$ the set of paths corresponding to the vertices of K. By Lemma 3, the grid segment $[x_0, x_2] \times \{y_0\}$ is covered only by vertices of K. For every $\lrcorner$-path (respectively, $\llcorner$-path) belonging to $\mathcal{P}_K$, we do the following. If the path does not intersect any path $P_t \notin \mathcal{P}_K$ on column x_1, then we delete its vertical segment and add the grid segment $[x_1, x_2] \times \{y_0\}$ (respectively, $[x_0, x_1] \times \{y_0\}$). If after this transformation there is no more $\lrcorner$-paths (respectively, $\llcorner$-paths) in $\mathcal{P}_K$, then we are done since we have obtained an edge-clique. So we may assume that every $\lrcorner$-path and every $\llcorner$-path in $\mathcal{P}_K$ intersects some path $P_t \notin \mathcal{P}_K$ on column x_1 (notice that we can assume there is the same path P_t for all the vertices). Since K is claw-clique, there is a path

$P_u \in \mathcal{P}_K$ covering the base of the claw. Thus, $G[v, v', u, t]$ induces a diamond, a contradiction. ■

An *independent set* of vertices is a set of vertices no two of which are adjacent. A graph G is said to be *bipartite* if its set of vertices can be partitioned into two distinct independent sets. There are bipartite graphs that are not B_1-EPG, for instance $K_{2,5}$ and $K_{3,3}$ (see [7]). Clearly, since bipartite graphs are triangle-free, any B_1-EPG representation of a bipartite graph is also a Helly-B_1-EPG representation. A similar result (but a bit weaker) is obtained as a corollary of the previous theorem.

Corollary 10. *If G is a bipartite* B_1-EPG *graph, then G is a* Helly-B_1-EPG *graph.*

Proof. The bipartite graphs are diamond-free, thus by Theorem 9 these graphs are Helly-B_1-EPG graphs. ■

A *block graph* or *clique tree* is a type of graph in which every biconnected component (block) is a clique.

Corollary 11. *Block graphs are* Helly-B_1-EPG.

Proof. Block graphs are known to be exactly the chordal diamond-free graphs, so by Theorem 19 of [3], all block graphs are B_1-EPG. If follows from Theorem 9 that all block graphs are Helly-B_1-EPG. ■

A *cactus* (sometimes called a cactus tree) graph is a connected graph in which any two cycles have at most one vertex in common. Equivalently, it is a connected graph in which every edge belongs to at most one cycle, or (for nontrivial cactus) in which every block (maximal subgraph without a cut-vertex) is an edge or a cycle. The family of graphs in which each component is a cactus is closed under graph minor operations. This graph family may be characterized by a single forbidden minor, the diamond graph.

Corollary 12. *Cactus graphs are* Helly-B_1-EPG.

Proof. In [6], it is proved that every cactus graph is a monotonic B_1-EPG graph (there is a B_1-EPG representation where all paths are ascending in rows and columns). Thus, cactus graphs are B_1-EPG graphs.

Since cactus are diamond-free, by Theorem 9, the proof follows. ■

Given a graph G, its *line graph* $L(G)$ is a graph such that each vertex of $L(G)$ represents an edge of G and two vertices of $L(G)$ are adjacent if and only if their corresponding edges share a common endpoint (i.e., are adjacent) in G. A graph G is a *line graph of a bipartite graph* (or simply *line of bipartite*) if and only if it

contains no claw, no odd cycle (with more than 3 vertices), and no diamond as an induced subgraph [16].

In [17] was proved that every line graph has a representation with at most 2 bends. We proved in the following corollary that when restricted to the line of bipartite we can obtain a Helly and 1-bended representation.

Corollary 13. *Line of bipartite graphs are* Helly-B_1-EPG.

Proof. Line of bipartite graphs were proved to be B_1-EPG in [14]. Since they are diamond-free, the proof follows from Theorem 9. ■

The diagram of Figure 5 illustrates the containment relationship among the graph classes studied so far in this work. We list in Figure 6 examples of graphs in each numbered region of the diagram. The numbers of each item below correspond to the regions of the same number in the diagram depicted in Figure 5.

(1) (B_1-EPG) - (Helly-B_1-EPG) graphs, depicted in Figure 6(a), graph E_1;

(2) (line of bipartite) - (cactus) - (block) - (bipartite) graphs, depicted in Figure 6(b), graph E_2;

(3) (Helly-B_1-EPG) - (line of bipartite) - (block) - (cactus) - (bipartite) graphs, depicted in Figure 6(c), graph E_3;

(4) (block) $\cap$ (line of bipartite) - (cactus) - (bipartite), depicted in Figure 6(d), graph E_4;

(5) (block) $\cap$ (line of bipartite) $\cap$ (cactus) - (bipartite), depicted in Figure 6(e), graph E_5;

(6) (cactus) $\cap$ (line of bipartite) - (block) - (bipartite). This intersection is empty. Let G be a graph that is cactus and line of bipartite then G is {claw, odd cycle, diamond}-free. But G is not a bipartite graph, then G has odd cycle, absurd with the hypothesis of G is line of bipartite;

(7) (bipartite) $\cap$ (line of bipartite) - (cactus) - (block) graphs, depicted in Figure 6(f), graph E_7;

(8) (bipartite) $\cap$ (line of bipartite) $\cap$ (cactus) - (block) graphs, depicted in Figure 6(g), graph E_8;

(9) (bipartite) $\cap$ (line of bipartite) $\cap$ (cactus) $\cap$ (block) graphs, depicted in Figure 6(h), graph E_9;

(10) (bipartite) $\cap$ (cactus) $\cap$ (block) - (line of bipartite) graphs, depicted in Figure 6(i), graph E_{10};

(11) (bipartite) $\cap$ (cactus) - (block) - (line of bipartite) graphs, depicted in Figure 6(j), graph E_{11};

(12) (bipartite) $\cap$ (Helly-B_1-EPG) - (cactus) - (block) - (line of bipartite) graphs, depicted in Figure 6(k), graph E_{12};

(13) (bipartite) - (B_1-EPG) graphs, depicted in Figure 6(l), graph E_{13};

(14) (block) - (bipartite) - (line of bipartite) - (cactus) graphs, depicted in Figure 6(m), graph E_{14};

(15) (block) ∩ (cactus) - (line of bipartite) - (bipartite) graphs, depicted in Figure 6(n), graph E_{15};

(16) (cactus) - (block) - (line of bipartite) - (bipartite) graphs, depicted in Figure 6(o), graph E_{16}, the odd cycles $C_{2n+1}, n \geq 2$;

(17) (Helly EPG) - (B_1-EPG) - (bipartite) graphs, depicted in Figure 6(p), graph E_{17};

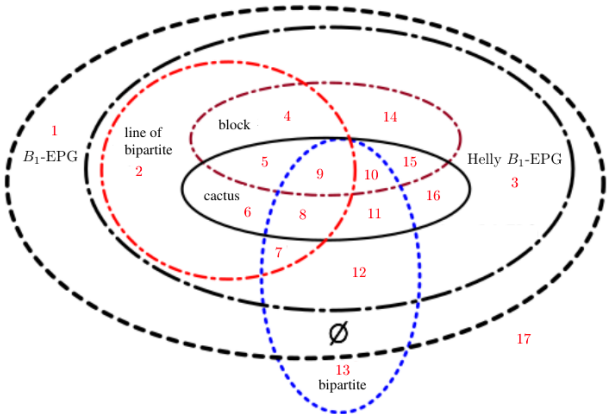

Figure 5. Diagram of some graph classes.

In the next section we explore the chordal B_1-EPG graphs through of a subset of forbidden graphs and we will prove that this class is in the strict intersection of VPT and EPT graphs.

4. Containment Relationship Among Chordal B1-EPG, VPT and EPT Graphs

Any graph that admits a B_1-EPG representation whose paths do not cover all the edges of a polygon of the grid (i.e., the subjacent grid subgraph is a tree) is also an EPT graph: the same representation is both B_1-EPG and EPT. However, it is easily verifiable that the subjacent grid subgraph of any B_1-EPG representation of a cycle C_n with $n \geq 5$ is not a tree, although C_n is an EPT graph. Our long-range goal is understanding the B_1-EPG graphs that are also EPT graphs. When can a B_1-EPG representation be reorganized into an EPT representation? In this section, we answer that question for chordal B_1-EPG graphs, in fact we prove that every chordal B_1-EPG graph is EPT. We made several unsuccessful attempts to

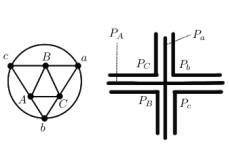

(a) Graph E_1.

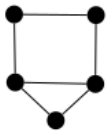

(b) Graph E_2.

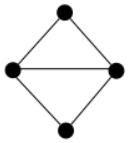

(c) Graph E_3.

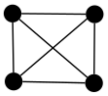

(d) Graph E_4.

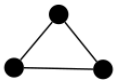

(e) Graph E_5.

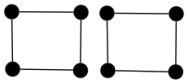

(f) Graph E_7.

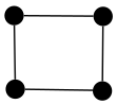

(g) Graph E_8.

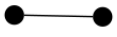

(h) Graph E_9.

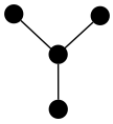

(i) Graph E_{10}.

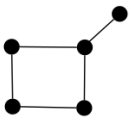

(j) Graph E_{11}.

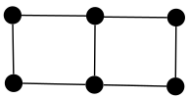

(k) Graph E_{12}.

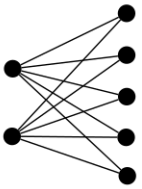

(l) Graph E_{13}.

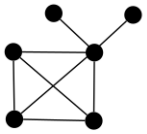

(m) Graph E_{14}.

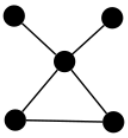

(n) Graph E_{15}.

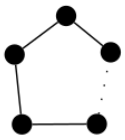

(o) Graph E_{16}, $C_{2n+1}, n \geq 2$.

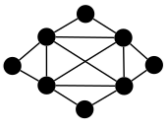

(p) Graph E_{17}.

Figure 6. The set of instances for the Venn diagram on Figure 5.

prove this result by considering for a graph G, a B_1-EPG representation whose paths cover all the edges of some polygon on the grid, and trying to show that if none of the paths could be modified in order to avoid an edge of the polygon, then G had some chordless cycle (i.e., G is not chordal). The surprise was that the only way we found to demonstrate our main Theorem 23 was through VPT graphs. We will prove the following theorem.

Theorem 14. *Chordal* B_1-EPG $\subsetneq$ VPT.

In Lévêque *et al.* [18] *apud* [2], VPT graphs were characterized by a family of minimal forbidden induced subgraphs, the ones depicted in Figure 7 plus the induced cycles C_n for $n \geq 4$. Therefore, in order to prove that chordal B_1-EPG graphs are VPT is enough to show that none of the graphs in Figure 7 is B_1-EPG.

First notice that in each one of the graphs F_1, F_2, F_3, F_4 and F_5 (Figures 7(a), (b), (c), (d), (e), respectively), the neighborhood of the universal vertex (the one that is a bit bigger than the others, in the respective figures) contains an asteroidal triple. Therefore, by Lemma 6, these graphs are not B_1-EPG.

Now, in each one of the graphs $F_{11}, F_{12}, F_{13}, F_{14}$, F_{15} and F_{16} (Figures 7(k),

(l), (m), (n), (o), (p), respectively), let C be the maximal clique in bold. It is easy to check that, in all cases, the branch graph $B(G|C)$ contains an induced cycle C_n, for some $n \geq 4$, or an induced path P_6; thus, by Lemma 7, graphs $F_{11}, F_{12}, F_{13}, F_{14}$, F_{15} and F_{16} are not B_1-EPG.

Observation 15. *Let e_ℓ, e_m and e_r be three distinct edges of a 1-bend path P, and assume that e_m is between e_ℓ and e_r on P. If P_ℓ and P_r are 1-bend paths such that: P_ℓ contains e_ℓ, P_r contains e_r, and P_ℓ and P_r intersect in at least one edge, then P_ℓ or P_r contains e_m.*

Observation 16. *Let e and q be an edge and a point of a 1-bend path P, respectively. If a 1-bend path P' contains both e and q, then P' contains the whole segment of P between q and e.*

Lemma 17. *Let G be a graph whose vertex set can be partitioned into a clique $K = \{a, b\}$ and an independent set $I = \{x, y, z\}$, such that each vertex of K is adjacent to each vertex of I. If in a given B_1-EPG representation of G, $P_a \cap P_y$ is between $P_a \cap P_x$ and $P_a \cap P_z$, then $\{a, b, y\}$ is an edge-clique, and $P_a \cap P_y \subset P_b$. Even more, any vertex adjacent to both a and y, but not to b (or to b and y, but not to a) has to be adjacent to x or to z.*

Proof. Assume in order to obtain a contradiction that $\{a, b, y\}$ is not an edge-clique. Then, by Lemma 5, we can assume, without loss of generality, that $\{a, b, x\}$ is an edge-clique. It implies that there is an edge e_ℓ of $P_a \cap P_x$ covered by P_b. Since every edge of $P_a \cap P_z$ is covered by P_z, z and b are adjacent, and z and y are non adjacent, we have by Observation 15, that every edge of $P_a \cap P_y$ is covered by P_b, which implies that $\{a, b, y\}$ is an edge-clique, contrary to the assumption.

Thus, $\{a, b, y\}$ is an edge-clique. By Observation 16, we have that the whole interval of P_a between $P_a \cap P_x$ and $P_a \cap P_z$ is contained in P_b, and so, in particular, $P_a \cap P_y \subset P_b$. Observe that this implies that if q is an end point of the interval $P_a \cap P_y$, and e is the edge of P_a incident on q that do not belong to P_y, then e belongs to P_b or to P_x or to P_z.

Now, assume there exists a vertex v adjacent to both a and y, but not to b. Then, the clique $\{a, y, v\}$ has to be a claw-clique. Let q be the center of the claw, notice that q has to be an end vertex of the interval $P_a \cap P_y$. Since v is not adjacent to b, it follows from the observation at the end of the paragraph above, that v has to be adjacent to x or to z. ∎

Lemma 18. *The graph F_6 in Figure 7(f) is not B_1-EPG.*

Proof. Let $K = \{1, 2\}$ and $I = \{3, 4, 5\}$. If there exists a B_1-EPG representation of F_6, by Lemma 17, because of the existence of the vertices 6, 7 and 8, none of the vertices 3, 4 and 5 may intersect 1 between the remaining two, thus such a representation does not exist. ∎

Lemma 19. *The graph F_7 in Figure* 7(g) *is not* B_1-EPG.

Proof. Let $K = \{1, 2\}$ and $I = \{4, 5, 6\}$. If there exists a B_1-EPG representation of F_7, by Lemma 17, because of the existence of the vertices 7 and 8, the vertex 6 must intersect vertex 1 between 3 and 4. But considering $K' = \{1, 3\}$, because of the existence of the vertices 5 and 6, vertex 4 must intersect vertex 1 between 5 and 6. This contradiction implies that such a representation does not exist. ■

Lemma 20. *The graphs F_8, F_9 and $F_{10}(8)$ in Figures* 7(h), (i) *and* (j), *respectively, are not* B_1-EPG.

Proof. Let $K = \{2, 3\}$ and $I = \{1, 6, 7\}$. If there exists a B_1-EPG representation of anyone of those graphs, by Lemma 17, because of the existence of the vertices 4 and 5, the vertex 1 must intersect 2 between the vertices 6 and 7. In addition, since $\{2, 6, 8\}$ is a clique, the vertex 8 intersects the vertex 2 in an edge of $P_6 \cap P_2$ (edge-clique) or in an edge incident to $P_6 \cap P_2$ (claw-clique). Analogously, because of the clique $\{2, 7, 8\}$, the vertex 8 intersects 2 in an edge of $P_7 \cap P_2$ (edge-clique) or in an edge incident to $P_7 \cap P_2$ (claw-clique). In any case, it implies that 8 intersects 2 on two different edges, each one in a different side of $P_2 \cap P_1$, thus, by Observation 16, 8 contains the interval $P_2 \cap P_1$, in contradiction with the fact that the vertices 1 and 8 are not adjacent. ■

Lemma 21. *The graphs $F_{10}(n)$ for $n \geq 8$ in Figure* 7(j) *are not* B_1-EPG.

Proof. The case $n = 8$ was considered in the previous Lemma 20, so assume $n \geq 9$. Let $K = \{2, 3\}$ and $I = \{1, 6, 7\}$. If there exists a B_1-EPG representation of anyone of those graphs, by Lemma 17, because of the existence of the vertices 4 and 5, the vertex 1 must intersect vertex 2 between 6 and 7. In addition, since $\{2, 6, 8\}$ is a clique, 8 intersects 2 in an edge of $P_6 \cap P_2$ (edge-clique) or in an edge incident to $P_6 \cap P_2$ (claw-clique). Analogously, because of the clique $\{2, 7, n\}$, n intersects 2 in an edge of $P_7 \cap P_2$ (edge-clique) or in an edge incident to $P_7 \cap P_2$ (claw-clique). In any case, it implies that 8 and n intersect 2 on two different edges, each one in a different side of $P_2 \cap P_1$. Therefore, there exist two consecutive vertices of the path $8, 9, \ldots, n$, say the vertices j and $j+1$, such that each one intersects P_2 on a different side of $P_2 \cap P_1$. Thus, by Observation 15, P_j or P_{j+1} must contain the interval $P_2 \cap P_1$, in contradiction with the fact that neither j nor $j + 1$ is adjacent to 1. ■

We have proved that every minimal forbidden induced subgraph for VPT is also a forbidden induced subgraph for chordal B_1-EPG. Moreover, there are graphs in VPT that do not belong to B_1-EPG, for instance the graph 4-sun S_4 is not in B_1-EPG, see [12], but it has a VPT representation, see Figures 8(a) and 8(b). Thus, VPT graphs properly contain chordal B_1-EPG graphs. This ends the proof of Theorem 14.

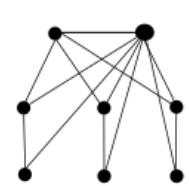

(a) Graph F_1.

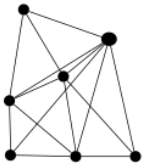

(b) Graph F_2.

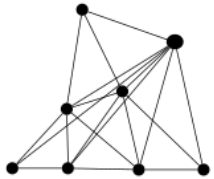

(c) Graph F_3.

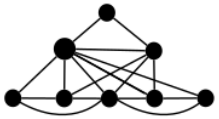

(d) Graph F_4.

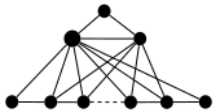

(e) Graph $F_5(n), n \geq 7$.

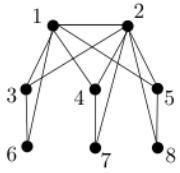

(f) Graph F_6.

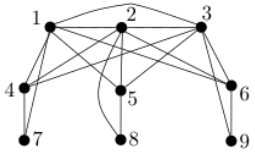

(g) Graph F_7.

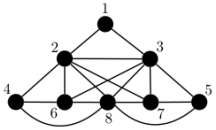

(h) Graph F_8.

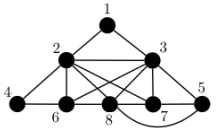

(i) Graph F_9.

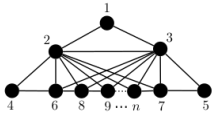

(j) Graph $F_{10}(n), n \geq 8$.

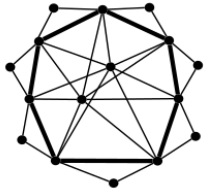

(k) $F_{11}(4k), k \geq 2$.

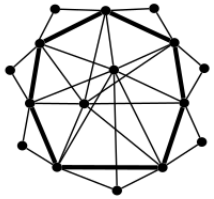

(l) $F_{12}(4k), k \geq 2$.

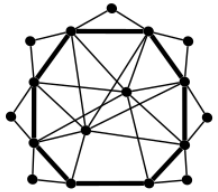

(m) $F_{13}(4k+1), k \geq 2$.

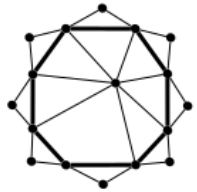

(n) $F_{14}(4k+1), k \geq 2$.

(o) $F_{15}(4k+2), k \geq 2$.

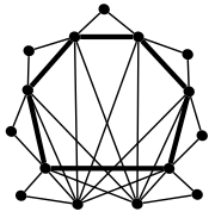

(p) $F_{16}(4k+3), k \geq 2$.

Figure 7. The 16 chordal induced subgraphs forbidden to VPT (the vertices in the cycle marked by bold edges form a clique).

Corollary 22. *Each one of the graphs depicted in Figure* 7 *is a forbidden induced subgraph for the class* B_1-EPG.

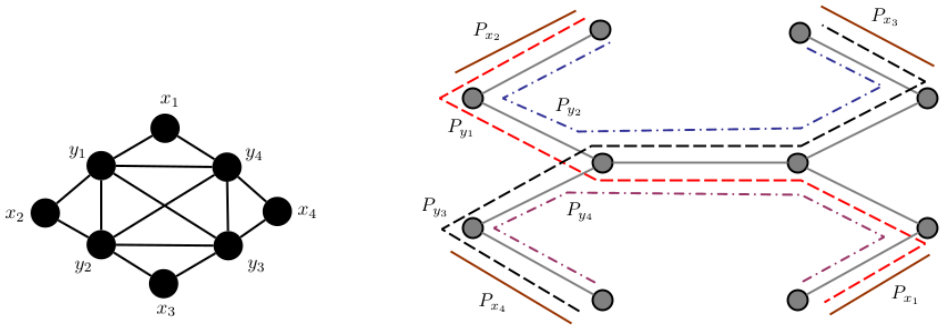

(a) Graph S_4. (b) A VPT and EPT representation of S_4.

Figure 8. Graph S_4 and one of its possible VPT and EPT representations.

Theorem 23. *Chordal* B_1-EPG $\subsetneq$ EPT.

Proof. Let G be a chordal B_1-EPG graph. By the previous Theorem 14, G is VPT. And, by Lemma 7, $\chi(B(G/C)) \leq 3$ for every maximal clique C of G. In [1] (see Theorem 10), it was proved that if the chromatic number of the branch graph of a VPT graph is at most h for every maximal clique, then the graph admits a VPT representation on a host tree with maximum degree h. Therefore, G admits a VPT representation on a host tree with maximum degree 3. Finally, in [10] (see Theorem 2), it was proved that any VPT graph that admits a representation on a host tree with maximum degree 3 is also an EPT graph. Consequently, G is EPT.

The same graph S_4 used in the proof of the previous theorem (see Figure 8(b)) shows that there are EPT graphs that are not B_1-EPG. ■

5. Conclusion and Open Questions

In this paper, we have considered three different path-intersection graph classes: B_1-EPG, VPT and EPT graphs. We showed that $\{S_3, S_{3'}, S_{3''}, C_4\}$-free graphs and others non-trivial subclasses of B_1-EPG graphs are Helly-B_1-EPG, namely by instance bipartite, block, cactus and line of bipartite graphs.

We presented an infinite family of forbidden induced subgraphs for the class B_1-EPG and in particular we proved that chordal B_1-EPG $\subset$ VPT $\cap$ EPT.

In [3], Asinowski and Ries described the split graphs that are B_1-EPG graphs in case the stable set or the central size have size three. The graphs $F_2, F_{11}, F_{13}, F_{14}$

and F_{15}, given in Figure 7 are split, we have used a different approach to prove that they are not B_1-EPG graphs. So one question is pertinent. Can we characterize split graphs in general based on the results of this paper?

Finally, another interesting research would be to explore families of Helly-EPG graphs more deeply. We would like to understand the behavior of other graph classes inside B_1-EPG graph class, i.e., if given an input graph G that is an instance of (for example) weakly chordal B_1-EPG. What is the relationship of G with the EPT/VPT graph class? What happens when we demand that the representations be Helly-B_1-EPG? Does recognizing problem remains hard for each one of these classes?

Acknowledgement

The present work was done while the third author was a doctoral research fellow at National University of La Plata - UNLP, Math Department. The support of this institution is gratefully acknowledged.

The third author (Tanilson) would like to thank the partial financing of this study by the Coordenação de Aperfeiçoamento de Pessoal de Nível Superior - Brasil (CAPES) - Finance Code 001.

References

[1] L. Alcón, M. Gutierrez and M.P. Mazzoleni, *Recognizing vertex intersection graphs of paths on bounded degree trees*, Discrete Appl. Math. **162** (2014) 70–77. https://doi.org/10.1016/j.dam.2013.08.004

[2] L. Alcón, M. Gutierrez and M.P. Mazzoleni, *Characterizing paths graphs on bounded degree trees by minimal forbidden induced subgraphs*, Discrete Math. **338** (2015) 103–110. https://doi.org/10.1016/j.disc.2014.08.020

[3] A. Asinowski and B. Ries, *Some properties of edge intersection graphs of single-bend paths on a grid*, Discrete Math. **312** (2012) 427–440. https://doi.org/10.1016/j.disc.2011.10.005

[4] A. Asinowski and A. Suk, *Edge intersection graphs of systems of paths on a grid with a bounded number of bends*, Discrete Appl. Math. **157** (2009) 3174–3180. https://doi.org/10.1016/j.dam.2009.06.015

[5] C.F. Bornstein, M.C. Golumbic, T.D. Santos, U.S. Souza and J.L. Szwarcfiter, *The complexity of Helly-B_1-EPG graph recognition*, Discrete Math. Theoret. Comput. Sci. **22** (2020) #19. https://doi.org/10.23638/DMTCS-22-1-19

[6] E. Cela and E. Gaar, *Monotonic representations of outerplanar graphs as edge intersection graphs of paths on a grid* (2019). arXiv:1908.01981

[7] E. Cohen, and M.C. Golumbic and B. Ries, *Characterizations of cographs as intersection graphs of paths on a grid*, Discrete Appl. Math. **178** (2014) 46–57. https://doi.org/10.1016/j.dam.2014.06.020

[8] F. Gavril, *The intersection graphs of subtrees in trees are exactly the chordal graphs*, J. Combin. Theory Ser. B **16** (1974) 47–56. https://doi.org/10.1016/0095-8956(74)90094-X

[9] F. Gavril, *A recognition algorithm for the intersection graphs of paths in trees*, Discrete Math. **23** (1978) 211–227. https://doi.org/10.1016/0012-365X(78)90003-1

[10] M.C. Golumbic and R.E. Jamison, *Edge and vertex intersection of paths in a tree*, Discrete Math. **55** (1985) 151–159. https://doi.org/10.1016/0012-365X(85)90043-3

[11] M.C. Golumbic and R.E. Jamison, *The edge intersection graphs of paths in a tree*, J. Combin. Theory Ser. B **38** (1985) 8–22. https://doi.org/10.1016/0095-8956(85)90088-7

[12] M.C. Golumbic, M. Lipshteyn and M. Stern, *Edge intersection graphs of single bend paths on a grid*, Networks **54** (2009) 130–138. https://doi.org/10.1002/net.20305

[13] M.C. Golumbic, M. Lipshteyn and M. Stern, *Single bend paths on a grid have strong Helly number* 4, Networks **62** (2013) 161–163. https://doi.org/10.1002/net.21509

[14] M.C. Golumbic, G. Morgenstern and D. Rajendraprasad, *Edge-intersection graphs of boundary-generated paths in a grid*, Discrete Appl. Math. **236** (2018) 214–222. https://doi.org/10.1016/j.dam.2017.10.014

[15] M.C. Golumbic and B. Ries, *On the intersection graphs of orthogonal line segments in the plane: characterizations of some subclasses of chordal graphs*, Graphs Combin. **29** (2013) 499–517. https://doi.org/10.1007/s00373-012-1133-7

[16] F. Harary and C. Holzmann, *Line graphs of bipartite graphs*, Rev. Soc. Mat. Chile **1** (1974) 19–22.

[17] D. Heldt, K. Knauer and T. Ueckerdt, *On the bend-number of planar and outerplanar graphs*, Discrete Appl. Math. **179** (2014) 109–119. https://doi.org/10.1016/j.dam.2014.07.015

[18] B. Lévêque, F. Maffray and M. Preissmann, *Characterizing path graphs by forbidden induced subgraphs*, J. Graph Theory **62** (2009) 369–384. https://doi.org/10.1002/jgt.20407

[19] M.M. Sysło, *Triangulated edge intersection graphs of paths in a tree*, Discrete Math. **55** (1985) 217–220. https://doi.org/10.1016/0012-365X(85)90050-0

Received 22 June 2020
Revised 18 March 2021
Accepted 22 March 2021